The Abdus Salam
International Centre for Theoretical Physics

United Nations
Educational, Scientific and
Cultural Organization

IAEA
International Atomic Energy Agency

2022-19

Workshop on Theoretical Ecology and Global Change

2 - 18 March 2009

Appendix

MOORCROFT Paul
Harvard University
Department of Organismic and Evolutionary Biology
26 Oxford Street, 02138 MA Cambridge
U.S.A.

Appendices

A. Leaf-level fluxes of carbon and water

The physiology sub-model provides values for the carbon flux per unit leaf area in μmol C m^{-2} s^{-1} when plants are not limited by below-ground resources, $A_o(z, \mathbf{x}, y, t)$, and when stomates and closed $A_c(z, \mathbf{x}, y, t)$, and the associated evaporative water loss per unit leaf area $\Psi_o(z, \mathbf{x}, y, t)$ and $\Psi_c(z, \mathbf{x}, y, t)$ respectively in μmol H_2O m^{-2} s^{-1}. Our implementation closely follows that of Foley *et al.* (1996).

A_o, A_c, Ψ_o and Ψ_c were calculated for each grid cell at 120 levels of shading, ranging from 100% to 0% of incoming Photosynthetically Active Radiation (PAR). The equations were forced with the ISLSCP Initiative I dataset 1°x1° 3-hourly near-surface climatological data (Meeson et al. 1995; Sellers et al. 1995) interpolated to hourly values of incoming short-wave radiation, air temperature (T_A), and mole fraction of water vapor in air for a representative day of each month. The hourly values of A_o, A_c, Ψ_o Ψ_c were then integrated over the entire month and converted into units of kgC m^{-2} y^{-1} and kgH_2O m^{-2} y^{-1} respectively. Thus for each month, we had a look-up-table with four columns (total A_o, A_c, Ψ_o, and Ψ_c for the month) and 120 rows (levels of shading).

The equation for A_o and A_c of C_3 photosynthesis is (Farquhar and Sharkey 1982)

$$\begin{aligned} A_o &= \min. \left\{ \begin{array}{c} \alpha L \frac{C_i - \Gamma}{C_i + \Gamma} \\ \frac{V_m (C_i - \Gamma)}{C_i + K_1 (1 + K_2)} \end{array} \right\} - V_m \gamma \\ A_c &= -\gamma V_m \end{aligned} \tag{A1}$$

where L is the absorbed PAR (μ Einsteins m^{-2} s^{-1}). Unless otherwise stated, we use functional forms and parameter values from Foley *et al.* (1996). The first term in the function above governs the light reaction of photosynthesis, with L equal to the flux density of PAR (Einsteins $m^{-2}s^{-1}$) and the second governs the dark reaction. C_i is the within-leaf concentration of CO_2 (mol mol^{-1}), α is the quantum efficiency (mol CO_2 Einstein $^{-1}$, 0.08 for C_3 plants), and Γ is the CO_2 compensation point (mol mol^{-1}).

We label the dimensionless temperature function $\epsilon(T|x, y)$ as:

$$\epsilon(T|x, y) = x e^{y(1/288.2 - 1/(T + 273.2))} \tag{A2}$$

where T is in degrees Celsius. This function equals x if $T = 15^o$ C. Here,

$$\Gamma = \epsilon(T_L|2.12 * 10^{-5}, 5000) \tag{A3}$$

where T_L is the temperature (°C) inside the leaf. In the dark reaction,

$$K_1 = \epsilon(T_L|1.5 * 10^{-4}, 6000) \tag{A4}$$

and

$$K_2 = \epsilon(T_L|0.836, -1400) \tag{A5}$$

Although V_m is often reported as the maximum capacity of Rubisco (μmol CO_2 m^{-2} s^{-1}), maximum photosynthetic capacity in the field is far below the ≈ 50 μmol m^{-2} s^{-1} that one would

expect from this definition. The value used by Foley *et al.* (1996) is 25 μmol m^{-2} s^{-1} (a value expected from RuP2 limitation (Mooney and Ehlerlinger 1997), but this is roughly double the average value as measured in the field on young sun leaves of hundreds of species Reich *et al.* (1997). Although leaves studied by Reich *et al.* might have been under some nitrogen limitation, the correlation between leaf nitrogen and maximum photosynthesis was not strong when expressed per unit leaf area. Moreover, maximum photosynthetic rates typically decline dramatically as leaves age (Mooney and Gulmon 1982), indicating additional limits on maximum photosynthetic capacity.

We set the value of V_m at the value suggested by the Reich *et al.* (1997) summary. Thus, V_m equals 12.5 μmol m^{-2} s^{-1} times a complex function of temperature:

$$V_m = 12.5 \frac{\epsilon(T_L|1.0, 3000)}{(1 + \mathrm{e}^{0.4(5.0-T_L)})(1 + \mathrm{e}^{0.4(T_L-45.0)})} \tag{A6}$$

The mechanistic numerator above is included for consistency with Foley *et al.* (1996), but it has little impact relative to the phenomenological denominator which causes V_m to increase rapidly from zero to approximately 12.5 μmol m^{-2} s^{-1} at 5^o C, and then decrease rapidly back to zero at 45^o C. Although phenomenological, this function captures large-scale patterns in measurements and is commonly used in land-surface parameterizations (for example (Bonan 1995) and (Sellers et al. 1986)).

Finally, leaf respiration is proportional to V_m with $\gamma = 0.02$. Our sub-model differs from that in Foley *et al.* (1996) in two other minor particulars. We omitted triose phosphate limitation of photosynthesis, and kept limitation as a strict "law of the minimum" rather than including the algebra that reduces the abruptness of transitions between the different types of limitation (light versus dark reactions), as neither of these had much effect.

The equations for C_4 photosynthesis are simpler than those for C_3:

$$\begin{aligned} A_o &= \min. \left\{ \begin{array}{c} \alpha L \\ V_m \\ 18000 V_m C_i \end{array} \right\} - \gamma V_m \\ A_c &= -\gamma V_m \end{aligned} \tag{A7}$$

where the notation is as before except $\alpha = 0.06$, $\gamma = 0.04$ and the temperature limitation of V_m is changed slightly by replacing 50^o C in the first term of the denominator of equation (A6) with 100° C.

Again following Foley *et al.* (1996), who followed Leuning (1995) and Ball *et al.* (1986), stomatal conductance c_s (μmol H_2O m^{-2} s^{-1}) is given as:

$$c_s = \frac{M A_o}{(C_i - \Gamma)(1 + D_s/D_o)} + b \tag{A8}$$

where M and b are the slope and intercept of the linear relation between c_s and A_o ($b = 0.01$ is cuticular conductance), $M = 8.0$ for C_3 and 4.0 for C_4, D_s is the difference between the mole fractions of water vapor in air inside and outside the leaf and D_o= 0.01 is a reference value (mol mol^{-1}). A simple diffusion one dimensional diffusion model implies:

$$A_o = \frac{c_s}{1.6}(C_A - C_i) \tag{A9}$$

$$\Psi_o = c_s D_s \tag{A10}$$

where Ψ_o is the rate of evaporation (μmol H_2O m^{-2} s^{-1}) and C_A is the CO_2 concentration in air (mol mol^{-1}). The denominator of 1.6 in equation (A9) converts stomatal conductance of water vapor into stomatal conductance of CO_2. Also, for simplicity, equations (A8), (A9) and (A10) assume that the boundary layer conductance is generally not limiting relative to c_s, although this assumption can be easily changed.

Because air inside leaves is always nearly saturated (Jarvis 1986), D_s is equal to the mole fraction of saturated air at the temperature inside the leaf e_L minus the mole fraction of water vapor in air surrounding the leaf e_a. The former quantity is given (in mol mol^{-1}) by:

$$e_L = (2.5414 \text{ x } 10^6)e^{(5415/(T_L+273.2))} \tag{A11}$$

The final equation describes the energy balance of the leaf:

$$R_n = \Lambda\Psi + \Theta(T_L - T_A) \tag{A12}$$

where R_n is absorbed short-wave radiation (J m^{-2} s^{-1}), Λ is the molar latent heat content of water vapor (J μmol^{-1}), T_A is air temperature, and Θ governs the rate of convective cooling. Although Θ will depend on leaf size, orientation and wind speed, here we choose the representative value of 38.4 J m^{-2} s^{-1} K^{-1} (Jarvis 1986, Grace 1998).

Equations (A1) or (A7) and (A8)-(A12) are solved simultaneously for: A_o, Ψ_o, c_s, T_L, C_i, and then for A_c, Ψ_c, C_i and T_L, after setting $c_s = b$ and substituting A_c and Ψ_c for A_o and Ψ_o in the equations. We then integrated the equations over each month and converted the values to kgC m^{-2} y^{-1} and kgH_2O m^{-2} y^{-1} as described above.

B. Below-ground Limitation of Leaf Physiology

In our model, low soil moisture and low available soil nitrogen limit leaf physiological performance of individuals causing their leaf-level carbon gain and water loss (A_n and Ψ) to move along a path between (A_o, Ψ_o) and (A_c, Ψ_c). The precise shape of this path will depend on the mechanisms of soil water and nutrient limitation within a plant. We thus follow Foley *et al.* (1996) and adopt a simple phenomenological interpolation scheme:

$$\begin{aligned} A_n(\bar{\mathbf{r}}, t, c^*) &= c^* A_o(\bar{\mathbf{r}}, t) + (1 - c^*) A_c(\bar{\mathbf{r}}, t) \\ \Psi(\bar{\mathbf{r}}, t, c^*) &= c^* \Psi_o(\bar{\mathbf{r}}, t) + (1 - c^*) \Psi_c(\bar{\mathbf{r}}, t) \end{aligned} \tag{B1}$$

where the degree of limitation, c^*, ranges from zero to one and depending on soil-water and nitrogen availability.

Each plant tissue in our model has a fixed C:N ratio. All the active pools ($B_a = B_r + B_{sw} + B_l$) have a common ratio $(C:N)_a$ that differs among functional types (see Plant Functional Diversity section below), and structural stem (B_s) has $(C:N)_s$ =150. Plants take up N from the available pool in the soil so as to maintain these ratios. If there is no available N, then c^* switches abruptly to zero, stopping carbon production. To avoid numerical problems, this switch is smoothed slightly as available N becomes very small.

Given available soil nitrogen, the value of c^* is : $c^* = 1/(1 + (D : S)_\Psi)$, where $(D : S)_\Psi$ is the ratio of water demand to water supply. Thus $c^* \approx 1$ if water supply greatly exceeds demand and $c^* \approx 0$ if the reverse is true.

The potential demand by a plant with leaf biomass B_l is $\Psi_o B_l l(\mathbf{x})$, where $l(\mathbf{x})$ is specific leaf area (m^2 kg^{-1}). We assume that supply is $K_W W B_r$, where K_W is a constant, W is available soil water, and B_r is root biomass. Thus; $(D : S)_\Psi = \Psi_o B_l l(\mathbf{x})/(K_W W B_r)$. The constant K_W is set to 80, chosen to cause stomatal closure near observed wilting points.

C. Plant Functional Diversity

The functional type vector $\mathbf{x}$ defines the characteristics of each plant functional type. It is comprised of two elements $[x_1, x_2]$. The first x_1 is discrete, specifying C_3 or C_4 physiology. The second x_2 is continuous, denoting the leaf life-span (yrs) of the plant type. The other physiological characteristics of the plant type are specified from its leaf life-span using the relationships shown in Figure 1a. We use Reich *et al.*'s (1997) regressions shown in left-hand panels of Figure 1a to specify the relationship between leaf longevity x_2 of the plant functional type and its specific leaf area (m^2 kg-C^{-1}): $l(\mathbf{x}) = 16.0 x_2^{-0.46}$ and leaf carbon-to-nitrogen ratio (g g^{-1}): $(C : N)_a = 27.8 x_2^{0.34}$. In addition to these physiological relationships, we specify two further relationships also shown in the two right hand panels of Figure 1a that define two attributes of plant structure. The first is an association between leaf-longevity and the wood density of the plant functional type (g cm^{-3}) $\rho(\mathbf{x}) = \max(0.5, 0.5 + 0.2(x_2 - 1))$, the second is an association between leaf longevity and maximum height (m) $(x_2 < 1 : h_{max} = 0.75, x_2 \geq 1 : h_{max} = 35$.

Together with these relationships, the functional type vector $\mathbf{x}$ specifies the physiological and life-history characteristics of a continuum of plant functional types. For the four functional types used in this paper, the values of the functional type vector $\mathbf{x}$ are: C_4 grasses ($x_1 = C_4, x_2 = 0.5$), early successional trees ($x_1 = C_3, x_2 = 1.0$), mid-successional trees ($x_1 = C_3, x_2 = 2.0$), and late successional trees ($x_1 = C_3, x_2 = 3.0$).

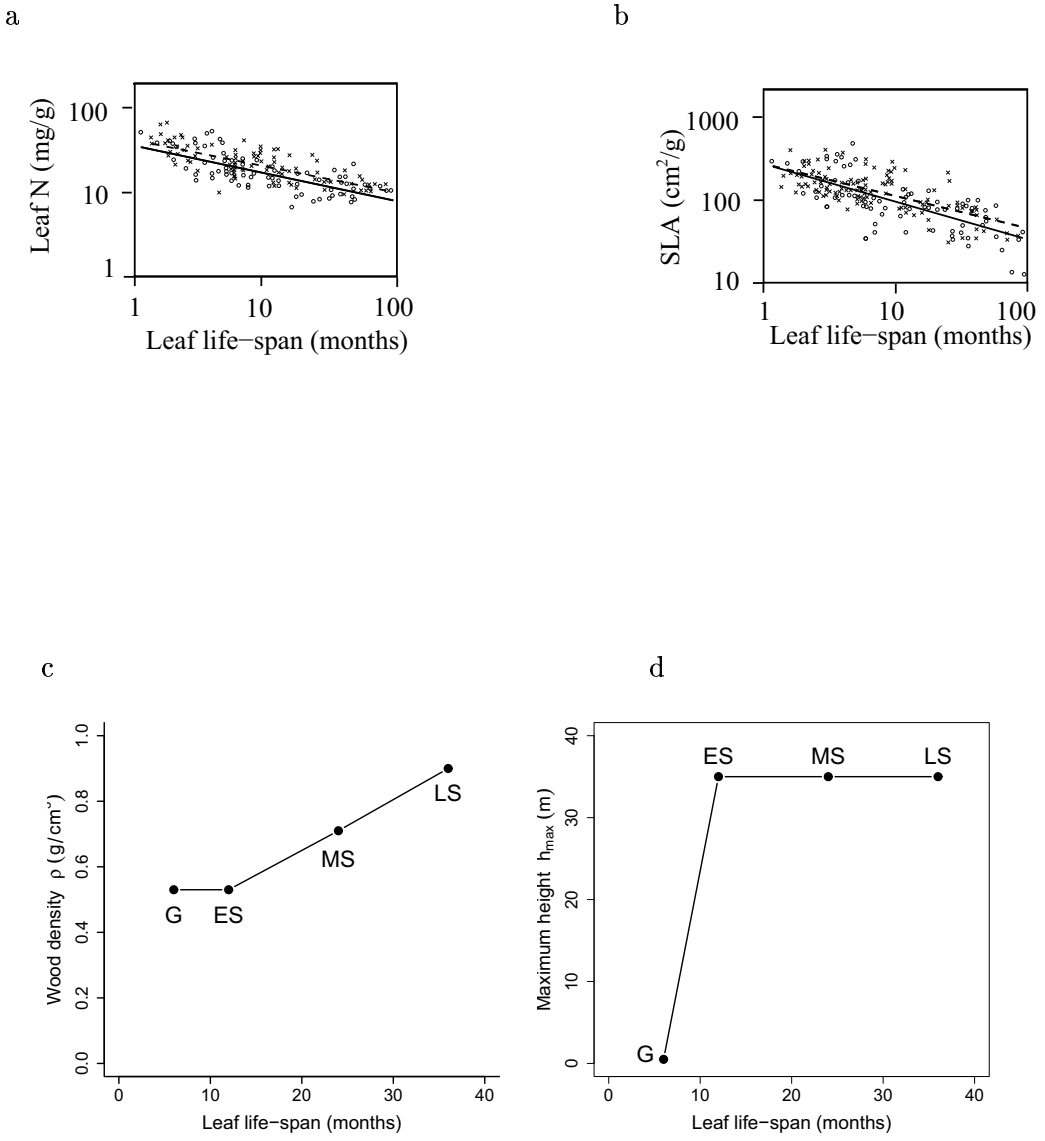

Figure 1a. Continuum of plant traits used to specify the characteristics of the plant functional types. Panels (a) and (b) show the correlated changes in leaf physiological characteristics identified by Reich *et al* (Reich et al. 1997) (a) Relationship between leaf nitrogen content and leaf longevity and (b), relationship between specific leaf area and leaf longevity (redrawn from (Reich et al. 1997)). Panels (c) and (d) show the associated variation in plant structural characteristics used to specify the plant-level properties of C_4 grasses (G), and early (ES), mid (MS) and late (LS) successional tree types. Panel (c) shows the relationship between wood density and leaf longevity and panel (d) shows the relationship between maximum size and leaf longevity.

D. Allocation and Allometry

We combined the height-diameter allometry from O'Brien *et al.* (1999):

$$h = 2.34D^{0.64} \tag{D1}$$

where D is diameter (cm) and h is height (m), with allometric data from Saldarriaga *et al.* (1988)

$$\begin{aligned} \text{if } h < h_{max} \quad B_l &= 0.0419 D^{1.56} \rho(\mathbf{x})^{0.55} \\ B_s &= 0.069 h^{0.572} D^{1.94} \rho(\mathbf{x})^{0.931} \\ \text{if } h \geq h_{max} \quad B_l &= 0.0419 D^{*1.56} \rho(\mathbf{x})^{0.55} \\ B_s &= 0.069 h_{max}^{0.572} D^{1.94} \rho(\mathbf{x})^{0.931} \end{aligned} \tag{D2}$$

where $\rho(\mathbf{x})$ is the wood density of the plant functional type and D^* is the diameter from the O'Brien *et al.* (1999) allometry corresponding h_{max}:

$$D^* = 0.265 h_{max}(\mathbf{x})^{1.56}. \tag{D3}$$

The empirical allometric relationships defined above are used define the trajectory of active and structural tissue growth. The total amount of active tissue carbon B_a^{opt} is given by the sum of its three components

$$B_a^{opt} = B_{sw} + B_l + B_r \tag{D4}$$

-see Figure 2. B_l is computed from the empirical relationships given in (D3) and B_{sw} and B_r are calculated in the following way. We assume that within each plant $B_r = B_l$ and a "pipe" model for amount of sapwood (specifies that a plant's sapwood cross-sectional area is proportional to its total leaf area (Shinozaki et al. 1964a; Shinozaki et al. 1964b))

$$B_{sw} = 0.00128 l(\mathbf{x}) B_l h. \tag{D5}$$

Plants in positive carbon balance (Prod > 0) allocate new production to grow along the empirical allometric relationships given above. This requires that they allocate a fraction $q_a(\mathbf{z}, \mathbf{x})$ of new carbon for growth to B_a and the remaining fraction $1 - q_a(\mathbf{z}, \mathbf{x})$ to B_s, where

$$q_a(\mathbf{z}, \mathbf{x}) = \frac{\frac{dB_a^{opt}}{dB_s}(B_s)}{1 + \frac{dB_a^{opt}}{dB_s}(B_s)}. \tag{D6}$$

and $\frac{dB_a^{opt}}{dB_s}$ is calculated using Eq.s (D1-D5).
In contrast, when in negative carbon balance, plants depart from this trajectory because their active compartment shrinks (due to tissue respiration and decay). Their inert structural compartment however, remains constant. If a plant with $B_a < B_a^{opt}$ subsequently comes back into positive carbon gain Prod > 0, it then allocates all production to regrowing its active tissues until it recovers the B_a^{opt} trajectory. Thus: $q_a(\mathbf{z}, \mathbf{x}) = 1$ if $B_a < B_a^{opt}$.

Finally, if $q_l(\mathbf{z}, \mathbf{x})$,$q_r(\mathbf{z}, \mathbf{x})$, and $q_{sw}(\mathbf{z}, \mathbf{x})$ are the fractions of B_a in leaf, root, and sapwood, respectively, then:

$$\begin{aligned} q_l(\mathbf{z}, \mathbf{x}) &= q_r(\mathbf{z}, \mathbf{x}) = \frac{1}{2 + 0.00128 l(\mathbf{x}) h} \\ q_{sw}(\mathbf{z}, \mathbf{x}) &= 1 - q_l(\mathbf{z}, \mathbf{x}) - q_r(\mathbf{z}, \mathbf{x}). \end{aligned} \tag{D7}$$

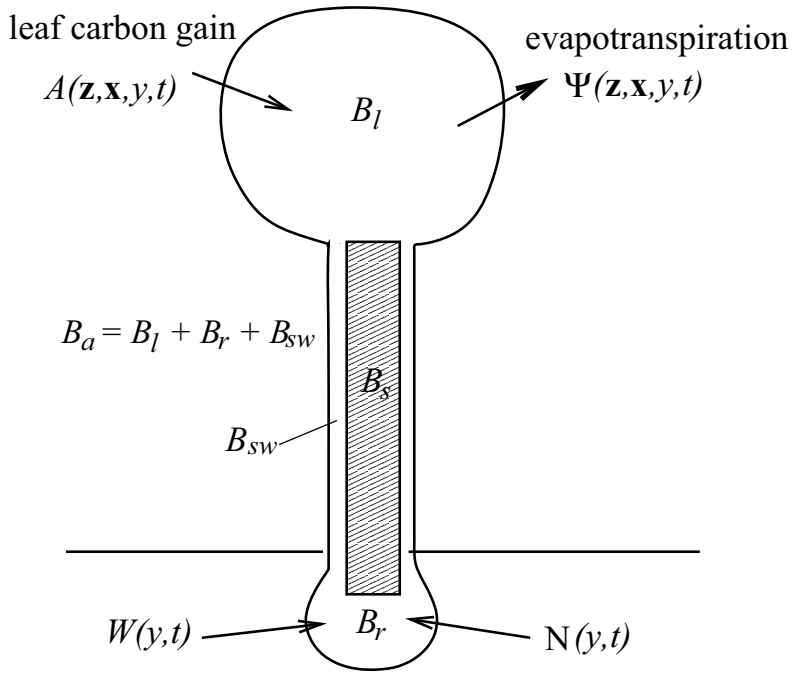

Figure 2. Individual-level fluxes of carbon, water and nitrogen and the partitioning of carbon between active and structural tissues (B_a and B_s respectively).

E. Growth and Reproduction

In this section, we define the growth and fecundity functions $g_s(\mathbf{z}, \mathbf{x}, \mathbf{r}, t)$, $g_a(\mathbf{z}, \mathbf{x}, \mathbf{r}, t)$ (both in kgC yr^{-1}) and $f(\mathbf{z}, \mathbf{x}, \mathbf{r}, t)$ (yr^{-1}). Because the derivation of these functions requires specification of the complete carbon budget for a plant, we will also define five additional quantities: per plant production ($\mathrm{Prod}(\mathbf{z}, \mathbf{x}, \mathbf{r}, t)$), per plant nitrogen lost through decay of leaves and roots ($N_{litter}(\mathbf{z}, \mathbf{x}, \mathbf{r}, t)$), per plant nitrogen uptake ($N_{up}(\mathbf{z}, \mathbf{x}, \mathbf{r}, t)$), per plant water uptake ($W_{up}(\mathbf{z}, \mathbf{x}, \mathbf{r}, t)$), and per plant carbon lost through decay of leaves and roots ($C_{litter}(\mathbf{z}, \mathbf{x}, \mathbf{r}, t)$). For notational convenience, note that unless specified otherwise, in this and subsequent Appendices, we have dropped the functional dependencies $(\mathbf{z}, \mathbf{x}, \mathbf{r}, t)$ of these per individual quantities. Note also that symbols not defined in this section have been defined in previous sections of the Appendix or the main text.

The total production by a plant's leaves, $A_n(\mathbf{r},t,c)l(\mathbf{x})B_l$, includes leaf respiration as well as photosynthesis (recall that $B_l = B_a q_a(\mathbf{z},\mathbf{x}), B_r = B_a q_r(\mathbf{z},\mathbf{x})$, and $B_{sw} = B_a q_{sw}(\mathbf{z},\mathbf{x})$). We assume that 30% of leaf production is lost as growth respiration (Amthor 1984), both structural and sapwood respiration is negligible and that instantaneous root respiration (kgC yr^{-1} per kgC roots) is given by

$$Resp = \frac{\epsilon(T_A|1.0,3000)}{(1+e^{0.4(5.0-T_A)})(1+e^{0.4(T_A-45.0)})}, \tag{E1}$$

which has the same form of temperature dependence as leaf respiration. This function is integrated over each month and placed into a look-up-table of monthly integrated root respiration rates.

Plants also lose carbon by the decay of leaves and fine roots at rate $\frac{1}{x_2}$ for leaves (the leaf decay rate is simply the reciprocal of leaf longevity) and α_r for fine roots, both in units kgC yr^{-1}. For simplicity we assume that sapwood decay is negligible and that $\alpha_r = \frac{1}{x_2}$. Versions with a constant value of α_r behave similarly.

There are now four cases to consider. First, suppose net plant-level production is positive. That is: Prod > 0, where

$$\text{Prod} \;=\; B_a[A_n(\mathbf{r},t,c^*)(1-\eta)l(\mathbf{x})q_l(\mathbf{z},\mathbf{x}) - q_r(\mathbf{z},\mathbf{x})Resp - \frac{1}{x_2}(q_l(\mathbf{z},\mathbf{x}) + q_r(\mathbf{z},\mathbf{x}))]. \tag{E2}$$

and $\eta = 0.3$ is the fraction lost as growth respiration.
Recall that all plants devote a fixed fraction F of positive net production to reproduction ($F = 0.3$) and $q_a(\mathbf{z},\mathbf{x})$ of the remaining fraction to growth of B_a and $1 - q(a)$ to growth of B_s. Thus

$$\begin{aligned} g_a(\mathbf{z},\mathbf{x},\mathbf{r},t) &= \text{Prod}(1-F)q_a(\mathbf{z},\mathbf{x}) && \text{(E3)}\\ g_s(\mathbf{z},\mathbf{x},\mathbf{r},t) &= \text{Prod}(1-F)(1-q_a(\mathbf{z},\mathbf{x})) && \text{(E4)}\\ f(\mathbf{z},\mathbf{x},\mathbf{r},t) &= F'\frac{\text{Prod}}{z_{s0}+z_{a0}} && \text{(E5)} \end{aligned}$$

where F' is F times germination and seedling survivorship probability ($s_0 = 0.05$) and $[z_{s0}, z_{a0}]$ is the size of a seedling.

We define $(\text{C:N})_{Prod}$ as the carbon-to-nitrogen ratio of an individual's new production:

$$\begin{aligned} (\text{C:N})_{Prod} &= [(1-F)q_a(\mathbf{z},\mathbf{x}) + Fq_a(\mathbf{z}_0,\mathbf{x})]\,(\text{C:N})_a \\ &\quad + [(1-F)q_s(\mathbf{z},\mathbf{x}) + Fq_s(\mathbf{z}_0,\mathbf{x})]\,(\text{C:N})_s. \end{aligned} \tag{E6}$$

Then:

$$\begin{aligned} N_{up} &= \frac{\text{Prod}}{(\text{C:N})_{Prod}} \\ C_{litter} &= \frac{1}{x_2}B_a(q_l(\mathbf{z},\mathbf{x}) + q_r(\mathbf{z},\mathbf{x})) \\ N_{litter} &= \frac{C_{litter}}{(\text{C:N})_a} \\ W_{up} &= \Psi(\mathbf{r},t,c^*)B_a q_l(\mathbf{z},\mathbf{x})l(\mathbf{x}). && \text{(E7)} \end{aligned}$$

Second, suppose that Prod < 0 and that soil moisture is above the critical threshold (W_{crit}) causing leaf drop. Because plants stop reproducing and producing structural stem if Prod < 0:

$$\begin{aligned} g_a(\mathbf{z},\mathbf{x},\mathbf{r},t) &= \text{Prod} && \text{(E8)} \\ g_s(\mathbf{z},\mathbf{x},\mathbf{r},t) &= 0 && \text{(E9)} \\ f(\mathbf{z},\mathbf{x},\mathbf{r},t) &= 0 && \text{(E10)} \end{aligned}$$

and:

$$\begin{aligned} N_{up} &= 0 \\ C_{litter} &= \frac{1}{x_2} B_a (q_l(\mathbf{z},\mathbf{x}) + q_r(\mathbf{z},\mathbf{x})) \\ N_{litter} &= \frac{\text{Prod}}{(\text{C:N})_a} \\ W_{up} &= \Psi(\mathbf{r},t,c^*) B_a q_l(\mathbf{z},\mathbf{x}) l(\mathbf{x}) && \text{(E11)} \end{aligned}$$

Third, suppose that soil moisture is beneath the critical threshold for leaf drop ($W(y,t) < W_{crit}$). Leaf carbon retained following leaf drop (see below) is held in a non-respiring, non-decaying pool but fine root respiration and decay continue. Thus:

$$\begin{aligned} g_a(\mathbf{z},\mathbf{x},\mathbf{r},t) &= -B_a q_r(\mathbf{z},\mathbf{x}) [Resp + \frac{1}{x_2}] && \text{(E12)} \\ g_s(\mathbf{z},\mathbf{x},\mathbf{r},t) &= 0 && \text{(E13)} \\ f(\mathbf{z},\mathbf{x},\mathbf{r},t) &= 0 && \text{(E14)} \end{aligned}$$

and:

$$\begin{aligned} N_{up} &= 0 \\ C_{litter} &= \frac{1}{x_2} B_a q_r(\mathbf{z},\mathbf{x}) \\ N_{litter} &= \frac{g_a(\mathbf{z},\mathbf{x},\mathbf{r},t)}{(\text{C:N})_a} \\ W_{up} &= 0 && \text{(E15)} \end{aligned}$$

Finally, if $W(y,t) = W_{crit}$, then instantaneous leaf drop occurs. We reset B_a to $B_a(1 - \frac{q_l(\mathbf{z},\mathbf{x})}{2})$ because plants re-translocate 50% of leaf carbon and nitrogen and an amount $B_a \frac{q_l(\mathbf{z},\mathbf{x})}{2}$ is added to the fast litter pool (see Appendix F). This instantaneous transition results in a step change in B_a when $W(y,t)$ falls below W_{crit}.

F. Mortality

The total mortality of plants is calculated as the sum of two terms

$$\mu(\mathbf{z},\mathbf{x},\mathbf{r},t) = \mu_{DI} + \mu_{DD} \qquad \text{(F1)}$$

The first component is an individual's density-independent mortality rate μ_{DI} (yr^{-1}) which is a linear function of it's wood density

$$\mu_{DI} = 0.014 + 0.15(1 - \frac{\rho(\mathbf{x})}{\rho(\mathbf{x}_{LS})}), \tag{F2}$$

where $\rho(\mathbf{x}_{LS}) = 0.9$ is the wood density of the late successional functional type. This function gives longevities consistent with empirical estimates, ranging from 15 years for the early successional tree type (Uhl and Jordan 1984) to 75 years for the late successional tree type (Swaine et al. 1987; Lugo and Scatena 1996). In the PDEs, we partition the μ_{DI} term into two pieces. The disturbance portion is

$$\lambda_{DI}(a,t) = 0.014 \tag{F3}$$

and the density independent mortality portion is:

$$\mu_{DI}(\mathbf{z},\mathbf{x},\bar{\mathbf{r}},t) = 0.15(1 - \frac{\rho(\mathbf{x})}{\rho(\mathbf{x}_{LS})}). \tag{F4}$$

The second mortality component is an individual's density-dependent mortality rate, which depends on the plant's current net carbon production (Prod from the previous section) relative to what it would be in full sun (Prod_{FS}):

$$\mu_{DD} = \frac{m_1}{1 + e^{(m_2 \frac{\mathrm{Prod}}{\mathrm{Prod}_{FS}})}} \tag{F5}$$

where $m_1 = 5.0$ and $m_2 = 10$.

G. Soil Hydrology

Local water availability $W(y,t)$ is calculated using a simple hydrology scheme describing vertical water fluxes in and out of a single soil layer with no horizontal coupling between adjacent areas

$$\frac{dW(y,t)}{dt} = \underbrace{P(t)}_{\text{precipitation}} - \underbrace{\sum_{i=1}^{R_y} W_{up}^{(i)}}_{\text{plant uptake}} - \underbrace{k\left[\frac{W(y,t)}{d\theta_{max}}\right]^{2\tau+2}}_{\text{percolation and runoff}}. \tag{G1}$$

where $W(y,t)$, is the local water availability per unit area in mm. While the precipitation rate $P(t)$ is uniform across the grid cell, water availability $W(y,t)$, is spatially heterogeneous, since total water uptake by within a gap y is influenced by the number of individuals within the gap R_y and their respective water uptake rates $W_{up}^{(i)}$, where the superscript $i = 1 \ldots R_y$ indicates the water uptake rate of the ith individual obtained from the growth sub-model (Equation (E7), (E11) or (E15), depending on current state of the plant).

Water losses due to percolation and runoff are described using Campbell's (1974) empirical formulation for hydraulic conductivity as function of soil texture and soil moisture content. The conductivity of the soil depends on the saturated hydraulic conductivity, k, the degree of saturation, $W(y,t)/d\theta_{max}$, where d is the soil depth and θ_{max} is the maximum soil moisture content; and τ, an empirical parameter governing the rate at which conductivity decreases as saturation levels decrease. The soil characteristics of each grid cell used in the hydrology sub-model equation were specified from the ISLSCP I gridded data of soil depth and texture compiled by Sellers *et al.* (Sellers et al. 1995), and the suggested hydrologic parameters for each soil texture class (see Table G). The monthly precipitation values $P(t)$ in Equation (G1) were specified from the ISLSCP I 1°x1° monthly precipitation dataset compiled by the Global Precipitation Climatology Centre GPCC (1993).

In the SAS approximation, Equation (G1) becomes

$$\frac{dW(a,t)}{dt} = \underbrace{P(t)}_{\text{precipitation}} - \underbrace{\int_{\mathbf{z}_0}^{\infty}\int_{-\infty}^{\infty} W_{up}(\mathbf{z},\mathbf{x},a,t)n(\mathbf{z},\mathbf{x},a,t)d\mathbf{x}d\mathbf{z}}_{\text{plant uptake}} - \underbrace{k\left[\frac{W(a,t)}{d\theta_{max}}\right]^{2\tau+2}}_{\text{percolation and runoff}} . \quad \text{(G2)}$$

and $W(a,t)$ becomes the second element of the resource vector $\bar{r}(\mathbf{z},\mathbf{x},a,t)$.

Table 1. ISLSCP Soil hydrology parameters.

Soil Type	θ_{max}	$K_{sat}(10^{-6}ms^{-1})$	τ
coarse	0.0363	14.1	4.26
medium/coarse	0.1413	5.23	4.74
medium	0.3548	3.38	5.25
fine/medium	0.1349	4.45	6.77
fine	0.263	2.45	8.17
organic	0.354	3.38	5.25

H. Organic-Matter Decomposition and Nitrogen Cycling

Our below-ground biogeochemical sub-model consists of five pools: a fast carbon pool C_1 (containing dead and decaying leaves, fine roots, and sapwood), a slow carbon pool C_2 (containing decomposing structural material), associated nitrogen pools N_1 and N_2, and a pool of mineralized plant available nitrogen N. The inputs to these pools consists of both litter from living plants and biomass from dead plants. The decomposition of organic matter in C_1 and C_2 mineralizes associated nitrogen in N_1 and N_2. Plants take up nitrogen from the pool of plant available nitrogen N. In the current implementation, the nitrogen budget of every gap is closed, and each gap is initialized with $N_1 = 1.0$, $N_2 = 0$, and $N = 1.0$ kgN m^{-2}.

For each gap y, our below-ground sub-model is:

$$\frac{dC_1(y,t)}{dt} = \sum_{i=1}^{R_y} C_{litter}^{(i)} + \sum_{i=1}^{R_y} C_{a,dead}^{(i)} - C_{1,decomp}(y,t) \quad \text{(H1)}$$

$$\frac{dC_2(y,t)}{dt} = \sum_{i=1}^{R_y} C_{s,dead}^{(i)} - C_{2,decomp}(y,t) \tag{H2}$$

$$\frac{dN_1(y,t)}{dt} = \sum_{i=1}^{R_y} N_{litter}^{(i)} + \sum_{i=1}^{R_y} N_{a,dead}^{(i)} - N_{1,min.}(y,t) \tag{H3}$$

$$\frac{dN_2(y,t)}{dt} = \sum_{i=1}^{R_y} N_{s,dead}^{(i)} - N_{2,min.}(y,t) \tag{H4}$$

$$\frac{dN(y,t)}{dt} = N_{1,min.}(y,t) + N_{2,min.}(y,t) - \sum_{i=1}^{R_y} N_{up}^{(i)} \tag{H5}$$

The variables $C_{litter}^{(i)}$, $N_{litter}^{(i)}$ are the carbon and nitrogen lost by the *ith* individual in the gap due to tissue decay, and $N_{up}^{(i)}$ is its rate of nitrogen uptake, obtained from the growth sub-model (Equation E7, E11 or E15, depending on current state of the plant) converted into per unit area rates (kg m^{-2} yr^{-1}) by dividing by the size of the gap 225m^2. $C_{a,dead}^{(i)}$ and $C_{s,dead}^{(i)}$, are fluxes of carbon into the fast and structural carbon pools caused by the probabilistic death of an individual i and $N_{a,dead}^{(i)}$ and $N_{s,dead}^{(i)}$ are the corresponding nitrogen inputs to the fast and structural nitrogen pools. $C_{a,dead}$, $C_{s,dead}^{(i)}$, $N_{a,dead}^{(i)}$, $N_{s,dead}^{(i)}$ are given by

$$\begin{aligned} C_{a,dead}^{(i)} &= \mu(\mathbf{z},\mathbf{x},\bar{\mathbf{r}},t)B_a, \\ C_{s,dead}^{(i)} &= \mu(\mathbf{z},\mathbf{x},\bar{\mathbf{r}},t)B_s, \\ N_{a,dead}^{(i)} &= \mu(\mathbf{z},\mathbf{x},\bar{\mathbf{r}},t)B_a/(\mathrm{C{:}N})_a, \\ N_{s,dead}^{(i)} &= \mu(\mathbf{z},\mathbf{x},\bar{\mathbf{r}},t)B_s/(\mathrm{C{:}N})_s, \end{aligned} \tag{H6}$$

where $\mu(\mathbf{z},\mathbf{x},\bar{\mathbf{r}},t)$ is the mortality rate of the individual (Equation F1) and the fluxes are converted to per unit area rates (kg m^{-2} yr^{-1}) by dividing by the gap area 225m^2. Finally, if $W(y,t) = W_{crit}$, then the material lost through leaf drop (see Appendix E) enters the below-ground carbon pools. An amount $B_a q_l(\mathbf{z},\mathbf{x})/2$ is added to $C_1(y)$ and an amount $B_a q_l(\mathbf{z},\mathbf{x})/(2(\mathrm{C{:}N})_a)$ is added to $N_1(y)$.

The decomposition rates $C_{1,decomp}(y,t)$ and $C_{2,decomp}(y,t)$ have intrinsically different decay times, which are modified by a common (0-1) function $A(y,t)$ of soil temperature, soil moisture, and potential evapotranspiration taken directly from the Century model (Parton et al. 1987) . The decomposition rates are:

$$C_{1,decomp}(y,t) = 11.0A(y,t)C_1(y,t), \tag{H7}$$

$$C_{2,decomp}(y,t) = 0.22A(y,t)C_2(y,t)c_{im}^*. \tag{H8}$$

Since nitrogen is mineralized during the decomposition of organic matter, the nitrogen mineralization rates $N_{1,min.}(y,t)$ and $N_{2,min.}(y,t)$ are directly proportional to the decomposition rates and are:

$$N_{1,min.}(y,t) = 11.0A(y,t)N_1(y,t), \tag{H9}$$

$$N_{2,min.}(y,t) = 0.22A(y,t)N_2(y,t)c^*_{im}. \tag{H10}$$

As equations (H8) and (H10) imply, the decomposition of high C:N structural material, and the associated nitrogen mineralization are halted if N becomes rare, analogous to the shutdown of plant photosynthesis by water and nitrogen limitation. Given available soil nitrogen, the value c^*_{im} is: $c^*_{im} = \frac{1}{(1+(D:S)_{im})}$ where $(D:S)_{im}$ is the immobilization demand for nitrogen relative to the supply of N. The demand for nitrogen in this process $D = 0.22A(y,t)C_2 * 0.65$ is calculated as the nitrogen necessary for a reduction in the C:N ratio of the decaying structural material from 150 to 10, and assuming a respiration of 30% (Parton et al. 1987). The supply of nitrogen is assumed to be proportional to available N in the soil ($S = \nu N$), with $\nu = 40$ set to a high value (relative to that of plants) under the assumption that microbes have greater access to available nitrogen than plants.

In the PDEs the terms in the below-ground sub-model equations (H1)-(H5) become integrals:

$$\begin{aligned}
\frac{dC_1(a,t)}{dt} &= \int_{-\infty}^{\infty}\int_{\mathbf{z}_0}^{\infty} n(\mathbf{z},\mathbf{x},a,t)C_{litter}(\mathbf{z},\mathbf{x},\bar{\mathbf{r}},t)d\mathbf{z}d\mathbf{x} \\
&+ \int_{-\infty}^{\infty}\int_{\mathbf{z}_0}^{\infty} n(\mathbf{z},\mathbf{x},a,t)C_{a,dead}(\mathbf{z},\mathbf{x},\bar{\mathbf{r}},t)d\mathbf{z}d\mathbf{x} - C_{1,decomp}(a,t) && \text{(H11)} \\
\frac{dC_2(a,t)}{dt} &= \int_{-\infty}^{\infty}\int_{\mathbf{z}_0}^{\infty} n(\mathbf{z},\mathbf{x},a,t)C_{s,dead}(\mathbf{z},\mathbf{x},\bar{\mathbf{r}},t)d\mathbf{z}d\mathbf{x} - C_{2,decomp}(a,t) && \text{(H12)} \\
\frac{dN_1(a,t)}{dt} &= \int_{-\infty}^{\infty}\int_{\mathbf{z}_0}^{\infty} n(\mathbf{z},\mathbf{x},a,t)N_{litter}(\mathbf{z},\mathbf{x},\bar{\mathbf{r}},t)d\mathbf{z}d\mathbf{x} \\
&+ \int_{-\infty}^{\infty}\int_{\mathbf{z}_0}^{\infty} n(\mathbf{z},\mathbf{x},a,t)N_{a,dead}(\mathbf{z},\mathbf{x},\bar{\mathbf{r}},t)d\mathbf{z}d\mathbf{x} - N_{1,min.}(a,t) && \text{(H13)} \\
\frac{dN_2(a,t)}{dt} &= \int_{-\infty}^{\infty}\int_{\mathbf{z}_0}^{\infty} n(\mathbf{z},\mathbf{x},a,t)N_{s,dead}(\mathbf{z},\mathbf{x},\bar{\mathbf{r}},t)d\mathbf{z}d\mathbf{x} - N_{2,,min.}(a,t) && \text{(H14)} \\
\frac{dN(a,t)}{dt} &= N_{1,min.}(a,t) + N_{2,min.}(a,t) - \int_{-\infty}^{\infty}\int_{\mathbf{z}_0}^{\infty} n(\mathbf{z},\mathbf{x},a,t)N_{up}(\mathbf{z},\mathbf{x},\bar{\mathbf{r}},t)d\mathbf{z}d\mathbf{x}. \\
& && \text{(H15)}
\end{aligned}$$

The reader may note that the $C_2 : N_2$ ratio is constant since all inputs to the structural decay pool have the same C:N (all structural material in the model has a C:N of 150), and since the mineralization of nitrogen in N_2 is linked to the decomposition of C_2. In contrast, the $C_1 : N_1$ ratio floats because different functional types in the model have different $(\text{C:N})_a$ (see Appendix C).

I. Fire

The probability that a fire occurs in a place depends generally on both the probability of local ignition events, and on the probability of the spread of fire from adjacent burning areas. Both dryness and fuel levels are important variables in these terms. We use a formulation that assumes fires are local in origin but that they spread across a landscape which is fine-grained. This is most accurate when fires are typically larger than the scale of gaps (15m x 15m), but much smaller than the scale of the grid cell (1°x1°).

We assume that the probability of fire in gap y is

$$\lambda_F(y,t)\Delta t = k_F \sum_{y=1}^{Q} \text{Fuel}(y,t) * \text{Ignition}(y,t)\Delta t, \tag{I1}$$

where Q is the number of gaps. Fuel is defined as total above-ground biomass (kgC m^{-2})

$$\text{Fuel}(y,t) = \sum_{i=1}^{R_y} (0.8B_s^{(i)} + 0.5(B_a^{(i)} + B_{sw}^{(i)})) \tag{I2}$$

where R_y is the number of plants in gap y. Ignition is implemented as a step function of local soil moisture

$$\begin{aligned} \text{Ignition}(y,t) &= 1 \text{ if } W(y) < W^*_{fire} \\ &= 0 \text{ otherwise.} \end{aligned} \tag{I3}$$

In the PDEs, we integrate to obtain the fire-disturbance rate

$$\begin{aligned} \lambda_F(a,t) &= k_F \int_0^\infty \int_{-\infty}^\infty \int_{\mathbf{z}_0}^\infty n(\mathbf{z},\mathbf{x},a,t)[0.8B_s(\mathbf{z},\mathbf{x},a,t) \\ &+ 0.5(B_a(\mathbf{z},\mathbf{x},a,t) + B_{sw}(\mathbf{z},\mathbf{x},a,t))]\text{Ignition}(\bar{\mathbf{r}},t)d\mathbf{z}d\mathbf{x}da, \end{aligned} \tag{I4}$$

where $\text{Ignition}(\bar{\mathbf{r}},t)$ is a delta function.

The two parameters in this fire model $k_F = 10$ and $W^*_{fire} = 200$mm were set to give reasonable landscape patterns of fire. The consequences of fire in this model are simple, all plants are killed and the carbon and nitrogen are transferred to the below-ground model.

*

References

Amthor, J. (1984). The role of maintenance respiration in plant growth. *Plant Cell and Environment 7*, 561–569.

Ball, J., I. Woodrow, and J. Berry (1986). A model predicting stomatal conductance and its contribution to the control of photosynthesis under different environmental conditions. Volume 4. Dordrecht, Netherlands: Martinus-Nijhoff.

Bonan, G. B. (1995). Land-atmosphere CO_2 exchange simulated by a land surface process model coupled to an atmospheric general circulation model. *Journal of Geophysical Research 100(D2)*, 2817–2831.

Farquhar, G. D. and T. D. Sharkey (1982). Stomatal conductance and photosynthesis. *Annual Review of Plant Physiology 33*, 317–345.

Foley, J. A., I. C. Prentice, N. Ramankutty, S. Levis, D. Pollard, S. Sitch, and A. Haxeltine (1996). An integrated biosphere model of land surface processes, terrestrial carbon balance, and vegetation dynamics. *Global Biogeochemical Cycles 10(4)*, 603–628.

(GPCC), G. P. C. C. (1993). Global area-mean monthly precipitation totals for the year 1988 (preliminary estimates, derived from rain-gauge measurements, satellite observations and numerical weather prediction results). Technical report, Offenbach.

Leuning, R. (1995). A critical appraisal of a combined stomatal-photosynthesis model for c_3 plants. *Plant Cell and Environment 18*, 339–355.

Lugo, A. and F. Scatena (1996). Background and catastrophic tree mortality in tropical moist, wet and rain forests. *Biotropica 28*, 585–599.

Meeson, B. W., F. E. Corprew, J. M. P. McManus, D. M. Myers, J. W. Closs, K. J. Sun, D. J. Sunday, and P. J. Sellars (1995). ISLSCP Initiative I - global data sets for land - atmosphere models, 1987-1988, CD. Technical report, NASA.

Mooney, H. and J. Ehlerlinger (1997). Photosynthesis. In *Plant Ecology*, pp. 1–27. Blackwell Science.

Mooney, H. and S. Gulmon (1982). Constraints on leaf structure and function in reference to herbivory. *Bioscience 32*, 198–206.

O'Brien, S., S. Hubbell, R. Condit, S. L. de Lao, and R. Foster (1999). Height, crown size and trunk diameter of 56 tree and shrub species in a neotropical forest. *(submitted)*.

Parton, W. J., D. S. Schimel, C. V. Cole, and D. S. Ojima (1987). Analysis of factors controlling soil organic matter levels in Great Plains Grasslands. *Soil Science Society of America Journal 51(5)*, 1173–1179.

Reich, P. B., M. B. Walters, and D. S. Ellsworth (1997). From tropics to tundra: global convergence in plant functioning. *Proceedings of the National Academy of Science USA 94*, 13730–13734.

Saldarriaga, J., D. C. West, M. L. Tharp, and C. Uhl (1988). Long-term chronosequence of forest succession in the upper Rio Negro of Colombia and Venezuela. *Journal of Ecology 76*, 938–958.

Sellers, P. J., B. W. Meeson, J. Closs, J. Collatz, F. Corprew, D. Dazlich, F. G. Hall, Y. Kerr, R. Koster, S. Los, K. Mitchell, J. McManus, D. Myers, K. J. Sun, and P. Try (1995). An overview of the ISLSCP Initiative I global data sets. In *ISLSCP Initiative I - global data sets for land - atmosphere models, 1987-1988, CD*. NASA.

Sellers, P. J., Y. Mintz, Y. C. Sud, and A. Dalcher (1986). A simple biosphere model (SiB) for use with general circulation models. *Journal of the Atmospheric Sciences 43(6)*, 505–531.

Shinozaki, K., K. Yoda, K. Hozumi, and T. Kira (1964a). A quantitative analysis of plant form -the pipe model theory. i. basic analyses. *Japenese Journal of Ecology 14*, 97–105.

Shinozaki, K., K. Yoda, K. Hozumi, and T. Kira (1964b). A quantitative analysis of plant form -the pipe model theory. ii. further evidence of the theory and its application in forest ecology. *Japenese Journal of Ecology 14*, 133–139.

Swaine, M., D. Lieberman, and F. Putz (1987). The dynamics of tree populations: a review. *Journal of Tropical Ecology 3*, 359–366.

Uhl, C. and C. Jordan (1984). Sucession and nutient dynamics following forest cutting and burning in amazonia. *Ecology 65*, 1476–1490.